ITS Reconstruction Tool-Suite: an inverse algorithm package for industrial process tomography

Kent Wei[1 2], ChangHua Qiu[1], Manuchehr Soleimani[2], and Ken Primrose[1]

[1] Industrial Tomography Systems Plc, Manchester, M3 3JZ, kent.wei@itoms.com
[2] Engineering Tomography Laboratory, University of Bath, Bath, BA2 7AY, m.soleimani@bath.ac.uk

ABSTRACT

Electrical resistance tomography (ERT) and electrical capacitance tomography (ECT) are two established process tomography techniques that can be applied into various indsutries. ERT can monitor the electrical conductivity changes in the process whereas ECT can detect the electrical dieletric materials. Due to their high-speed and low cost features, they are particularly attractive to industrial applications which require real time conditional monitoring. For the past decades, 2D linear back projection (LBP) has been the standard technique for both commercialised ERT and ECT systems because of its simplicity and fast reconstruction speed. In this paper, ITS Plc has released a 'Reconstruction Tool-Suite' software that allows industrial users to utilise different reconstruction algorithms to further understand their processes. Different algorithms are integrated into this software package including the single stepTikhonov method and the iterative Landweber method. In the latest version of the software, the full-field 3D tomography reconstruction scheme is also included, which allows the users to perform 3D reconstruction for their processes. A series of experiments are conducted to validate the pros and cons of different methods.

Keywords ERT, ECT, Reconstruction Algorithms, Inverse methods

1. INTRODUCTION

Electrical Tomography is a measuring technique that can visualise the electrical properties of the imaging object. Electrical resistance tomography (ERT) and electrical capacitance tomography (ECT) are two the most established electrical tomography techniques, where ERT has the ability of visualise the conductivity properties of the process, and ECT is able to visualise the permittivity distribution within the sensor. Electrical tomography has advantages of low cost and high speed. The technique can offer qualitative information; therefore it is particularly attractive to many industrial applications. Since 1980s, when the electrical tomography technique was first invented [Henderson 1978; Barber 1984], considerable amount of work has been done on both ERT and ECT fields, and the techniques have been applied to many industrial applications such as fluid mixing monitoring [Rodgers 2010], oil / gas distributions [Gamio 2005] and slug in water detection [Giguére 2008].

Up to now, the linear back projection (LBP) method has been the standard reconstruction algorithm for commercialised ERT and ECT. LBP is popular for electrical tomography applications because of its simplicity for mathematical computation; it does not require other regularisation in the model and hence it can offer a very good temporal resolution. And also, because of the simplicity, 2D electrical modelling has also been the main approach for tomography applications, i.e. the conductivity/permittivity distributions are shown using 2D cross sectional slices, assuming there is no axial variation in the process. However, due to the nature of electro-magnetic field, the electrical tomography technique can potentially be expanded to 3D application [Wang 1999].

For the past two decades, there have been many researches on image reconstruction optimisation and 3D tomography modelling to generate a more accurate tomogram. Many researchers have proposed real three dimensional conductivity imaging [Davidson 2004; Sun 2012] and permittivity imaging [Soleimani 2006; Wajman 2006; Fan 2007; Banasiak 2010; Yan 2013] reconstruction methods, to achieve a better understanding of industrial processes. Sometimes with a fast sampling speed system, 2.5D images can also be achieved, by stacking several 2D images together [Ye 2012]. Nevertheless, these research outcomes are mainly kept within the academic researches and not yet available for the industrial users.

Industrial Tomography Systems plc (ITS) is the world leader in process tomography techniques. In this paper, a Reconstruction Tool-Suite software developed by ITS will be presented. The program

integrates some most popular image reconstruction methods and will be available for all ITS customers (ERT and ECT) to provide further insight about their processes, in both 2D and 3D manners. The new algorithms available in the software are: Tikhonov, NOSER, Laplace, and Landweber methods. From the literature, it is known that the regularised algorithms often require more computational resource and time than LBP (it is the reason why LBP is still the main method for industrial electrical tomography applications). In this Reconstruction Tool-Suite package, the 'Super Jacobian' scheme is implemented, which can massively reduce the computational resources for the new algorithms. Moreover, with the 3D reconstruction capability, ITS tomography user can analyse their process in a more complete manner, because the axial information is now also provided in the tomograms. The detail of the program development will be discussed in this paper.

2. SOFTWARE DEVELOPMENTS

2.1 Forward Algorithms

In electrical tomography, forward models are the physical simulations that predict the sensor measurements based on the electrical distribution within tomography sensors. The forward problems of are mainly solved by the Maxwell's equation, assuming that the time-harmonic field with angular frequency ω is implemented to the Maxwell's equation. Since the electrical tomography is considered as near field models, the propagation effect is ignored in the Maxwell's equation. When solving forward models, finite element methods (FEM) are usually used for discretisation of the sensing region. The 2D forward models [Lionheart 2004; Soleimani 2005] and 3D forward models [Soleimani 2007; Marashdeh 2004; Xu 2005] of ERT and ECT are discussed thoroughly in the literature. The detail will not be discussed here because it is beyond the scope of this paper.

2.2 Inverse Algorithms

The inverse problems are the algorithms that convert the sensor measurements into the electrical property distribution, which are utilised heavily in the Reconstruction Tool-Suite. Inverse problems for electrical tomography are challenging because of two difficulties. Firstly, the equations are under-determined, i.e. the number of unknown (pixel numbers in one tomogram) is often much larger than the number of sensor measurements. Therefore, the inverse solution will not be unique. Secondly, due to the nature of electro-magnetic distribution, the inverse problem is considered severely ill-posed, i.e. the inverse solution will be very sensitive to small perturbation of system noise. In the same way, a tiny voltage measurement change at the boundary can cause a large change in the computed conductivity distribution. For the past decades, Inverse algorithms for ERT and ECT have been reviewed extensively [Lionheart 2004; Yang 2003], all the developed algorithms are aiming to overcome the previously mentioned challenges.

In ITS Reconstruction Tool-Suite, five reconstruction methods are included in the package (see Table 1). All the algorithms are available in literature and public domain. In general, all the reconstruction methods are solving the linear equation $Ax = b$, where A is the Jacobian matrix, x is the conductivity/permittivity change and b is the voltage measurement.

Inverse Algorithms	Formula	References
Linear Back Projection	$x = A^{\mathrm{T}}b$	Lionheart 2004, Yang 2003
Tikhonov	$x = (A^{\mathrm{T}}A + \alpha_I I)^{-1}A^{\mathrm{T}}b$, where α_I is the Tikhonov regularisation parameter and I is an identity matrix	Lionheart 2004, Yang 2003
NOSER	$x = (A^{\mathrm{T}}A + \alpha_N N)^{-1}A^{\mathrm{T}}b$, where α_N is the NOSER regularisation parameter and N is the NOSER diagonal matrix	Cheney 1990, Dai 2008
Laplace	$x = (A^{\mathrm{T}}A + \alpha_L L)^{-1}A^{\mathrm{T}}b$, where α_L is the Laplace regularisation parameter and L is Laplacian filter matrix	Adler 2006
Landweber	$x_{k+1} = x_k + \alpha A^{\mathrm{T}}(b - Ax_k)$, where α is the Landweber relaxation factor and k indicates the number of iterations	Lionheart 2004, Yang 2003

Table 1: Algorithms available in ITS Reconstruction Tool-Suite

All the new reconstruction methods utilise a technique called ‘regularisation’ to overcome the ill-posed features of ERT and ECT. They are used to help the inverse solver finding the solution based on the prior constraint information. Different regularisations provide different constraints to the inverse solver; therefore different regularisation parameters are required for different algorithms. At the same time, however, providing incorrect constraints to the solver may introduce artefacts into tomograms.

One must note that the inverse solution strongly depends on the regularisation parameter. A careful selection of the parameter value is essential for an optimised reconstruction process. In the reconstruction Tool-Suite, a pre-selected regularisation values are provided in the software, which can help the software user achieving the best tomographic result.

2.3 C++ Implementation

2.3.1 Software Architecture

Figure 1 shows the software structure of and the graphical user interface (GUI) architecture of Reconstruction Tool-Suite. C++ is selected as the kernel language because it is good for real time data processing. The program also implements the View/Doc architecture from Microsoft Foundation Classes (MFC) to ease the file I/O support. MFC can also support software GUI, the main process of the software that interacts with users.

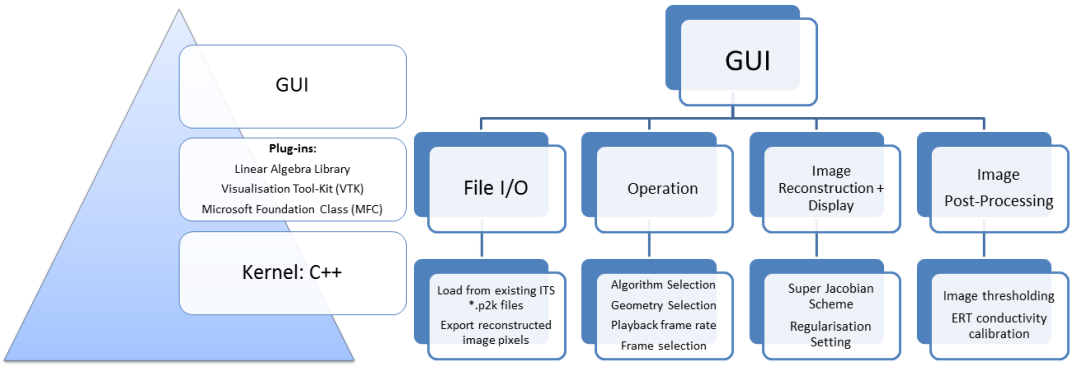

Figure 1: The Reconstruction Tool-Suite architecture and its GUI structures

Reconstruction Tool-Suite GUI must be able to read the measurement file, display the reconstructed images and store the result. Figure 2 shows the designed Reconstruction Tool-Suite GUI. In order to handle the GUI events received from the user, a number of plug-in libraries must be used. By calling the built-in functions in the libraries, these tasks can then be executed successfully. For example, to inherit the file format (*.p2k) from the previous ITS Tomography Tool-Suite software, the file structure is required when developing the software I/O utility. To solve the inverse problem, a linear algebra library is required to ease the matrix calculation. There are several linear algebra libraries available online, selecting an appropriate library is vital for the software development as image reconstruction processes utilise linear algebra calculations extensively. The library selection process will be discussed in the next section.

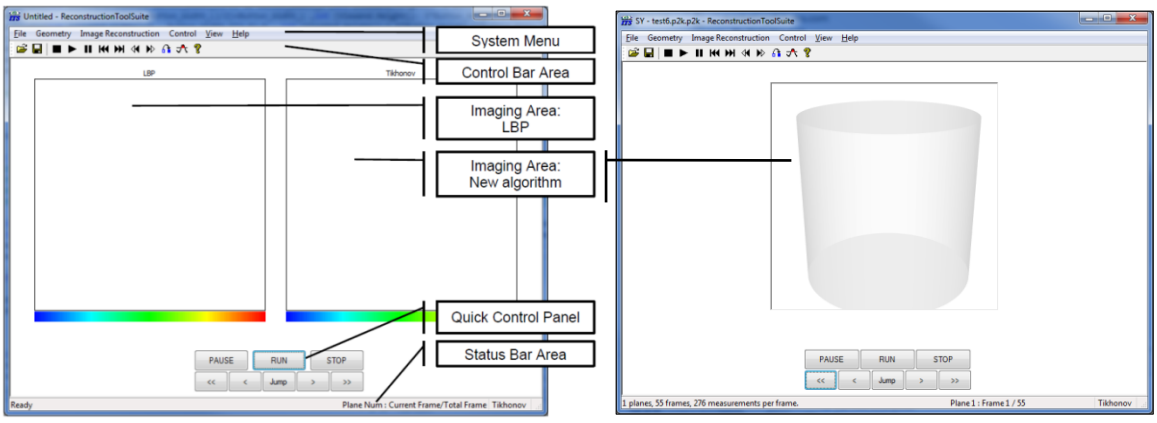

Figure 2: A screenshot of Reconstruction Tool-Suite GUI for (left) 2D and (right) 3D operations

2.3.2 C++ Linear Algebraic Libraries

From Section 2.2, it can be seen that all the inverse algorithms are based on linear algebraic calculations. There are several free linear algebra libraries available. Table 2 is a summary table about the free libraries which are currently active [LAPACK 2014; Armadillo 2014; Eigen 2014].

Library Name	Latest Release	Features
LAPACK (Linear Algebra Package)	Version 3.5.0 (November 2013)	**Pros**: Stable and Mature algorithms. Complete matrix solving functions. **Cons**: Ported from Fortran language, the API usage is not very straightforward.
Eigen C++	Eigen 3.2.2 (Aug 2014)	**Pros**: Clean API, easy to use. Low memory overhead with highly performant matrix solving kernel. **Cons**: Fewer geometric/rendering specific routines.
Armadillo C++	Version 4.500 (Oct 2014)	**Pros**: Intuitive interface and the syntax are similar to MATLAB. It contains wide range of decompositions functions. **Cons**: It is BLAS/LAPACK dependent.

Table 2: Comparison table of free linear algebraic libraries

Eigen library is selected for matrix calculation because of its completely self-contained feature, i.e. the library is independent of any external function. Before implementing the library into the software, the Eigen reconstruction result is cross-checked with the MATLAB result for performance evaluation. Figure 3 shows the sample ECT images reconstruction by using C++ Eigen library and MATLAB. Although different decomposition libraries were used for matrix inversion, it can be seen that the image shape are pretty much corresponding to each other.

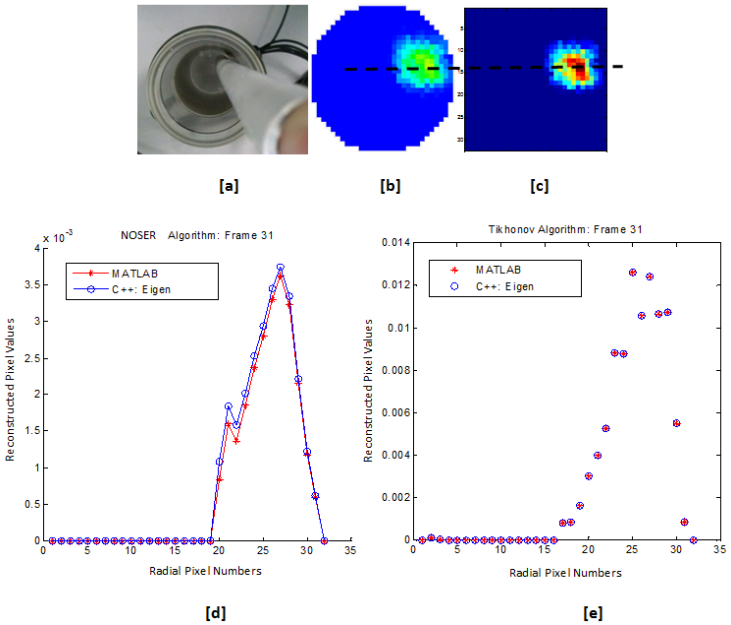

Figure 3: Reconstruction results using C++ Eigen and MATLAB linear algebra library. (a) The real case, (b) reconstructed Tikhonov image using Eigen library, (c) reconstructed Tikhonov image using MATLAB, (d) the cross section comparison using NOSER algorithm, (e) the cross section comparison using Tikhonov algorithm

2.3.3 Super Jacobian Scheme

From the literature, it is known that the regularised methods such as Tikhnov, NOSER and Laplace require extra computational resource than LBP because of the extra $(A^{\mathrm{T}}A + \alpha_R R)^{-1}$ calculation (see Table 1), where α_R is the regularisation parameter, A is the sensitivity matrix and R is the regularisation matrix. This extra matrix multiplication and decomposition process massively increases the computational cost and the calculation time. This is mainly the reason why the regularised method

like Tikhonov is generally avoided by the industrial user, as the method is not suitable for online calculation.

In the Reconstruction Tool-Suite, a 'Super Jacobian' scheme is proposed to make the single step regularised methods to run as fast as the LBP method. The aim of the Super Jacobian scheme is to avoid the expensive $(A^{\top}A + \alpha_R R)^{-1}$ computation. To calculate the Super Jacobian S, the regularisation parameter needs to be known in prior:

$$x = Sb, \text{ where } S = (A^{\top}A + \alpha_R R)^{-1}A^{\top}$$

For the 3D single step reconstruction, the $A^{\top}A$ calculation needs to be avoided because of its large memory consumption. The equation above can be modified using the Wiener filter scheme [Adler 2007]:

$$x = Sb, \text{ where } S = A^{\top}(AA^{\top} + \alpha_R R)^{-1}$$

After S is calculated, this Super Jacobian matrix will be stored in the stack memory for future inverse calculation, provided that the regularisation level remains the same. Once α_R and R are defined, the Super Jacobian matrix S can be calculated. Thereafter the $x = Sb$ calculation will consume the same amount of memory as the ordinary LBP calculation. Once the Super Jacobian matrix is calculated, if the regularisation parameter remains the same, Super Jacobian S can be re-used for the inverse solver and hence avoid the redundant calculation and therefore, reduce the computation cost.

However, this Super Jacobian scheme can only be applied to the single step methods such as Tikhonov, NOSER and Laplacian methods. For iterative method such as Landweber, the scheme cannot be applied because this iterative solver does not involve $(A^{\top}A + \alpha_R R)^{-1}$ calculation.

2.3.3 3D Visualisation

After the conductivity/permittivity voxel values are calculated, an interactive 3D visualisation library is required in order to provide more valuable information about the industrial process. Some 3D visualisation effect, for example, 360 degrees angular rotation, zoom-in and zoom-out…etc, these functions allow tomography users to understand their industrial process further, aiming to improve their process efficiency.

Visualisation Tool Kit (VTK) is an open source, free available C++ library for 3D graphics, imaging processing and visualisation. The strength of VTK library is its ability to represent complex form of data. Due to the nature of the forward problem, mesh information is often required for visualisation; using VTK library can easily handle those complex finite element mesh structures. VTK implements the pipeline architecture for data visualisation; Figure 3 shows a simplified pipeline structure. By applying different functions in different blocks, different images will be presented at the end of the pipeline. For example, for the conducted 3D experiments (in Section 4), there are always clear boundary changes of conductivity/permittivity distribution. Therefore an iso-surface image can best represent the 3D result. In order to produce an iso-surface image from a source data, a vtkContourFilter() needs to be applied to the pipeline to extract the contour pixels, and the filtered data will then be fed into a vtkPolyDataMapper() to convert the data into a tangible object for visualisation. Actors and renderers are used to adjust the visualisation properties of the object, such as transparency, colour, viewing direction…etc).

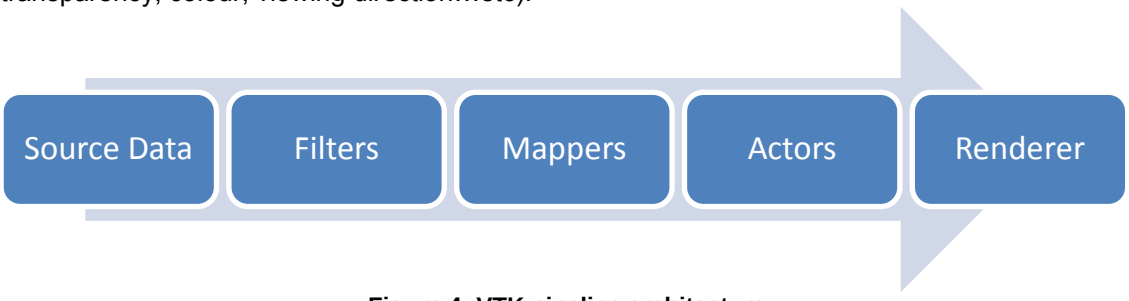

Figure 4: VTK pipeline architecture

3. EXPERIMENTAL VALIDATIONS – 2D

To verify the developed Tool-Suite, several benchmarking experiments were designed using ITS tomography instrumentation and sensors. The measurements of the ECT and ERT data were carried out by using the ITS M3C and P2+ system respectively (Figure 5).

Figure 5: ITS m3c ECT instrument and p2+ ERT instrument

3.1 ECT Experiments

The sensor used for ECT experiments is a 12 channel cylindrical sensor, with a diameter of 4.7mm. In the first test, the sensor pipe was placed in horizontal position, and different volumes of polypropylene beads were placed inside the sensor to detect the polypropylene/air interface. Figure 6 shows the reconstructed images using different inverse algorithms.

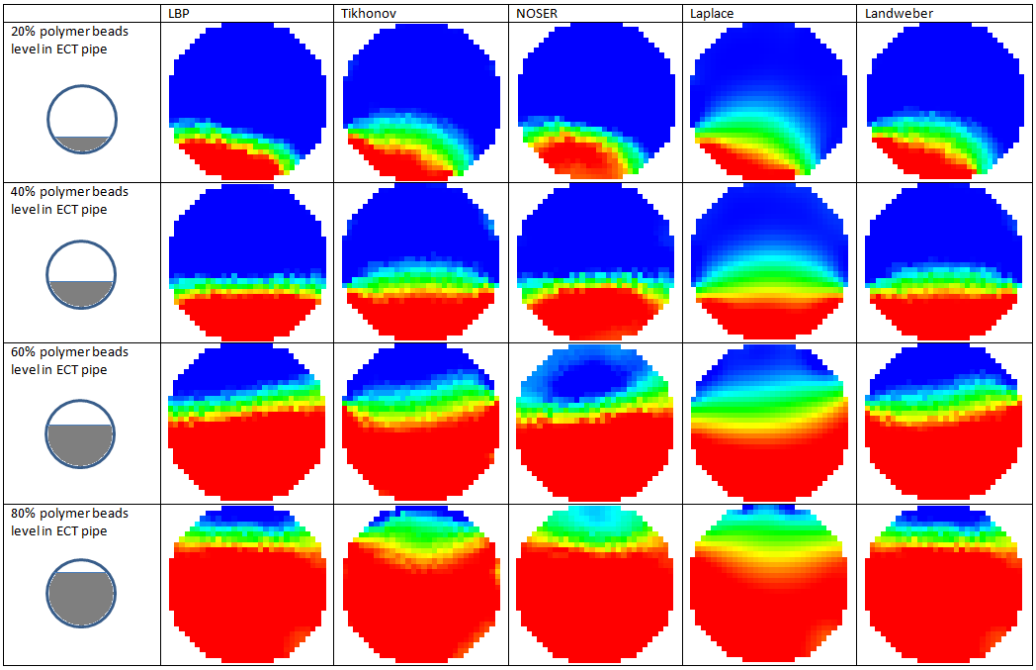

Figure 6: The ECT interface detection experiment for 20%, 40%, 60% and 80% of the polymer beads in an ECT sensor pipe

In the second test, an L shape plastic object was inserted into the same sensor. The aim of this test is to find out the shape recovery ability for different algorithms. Figure 7 gives the reconstruction result.

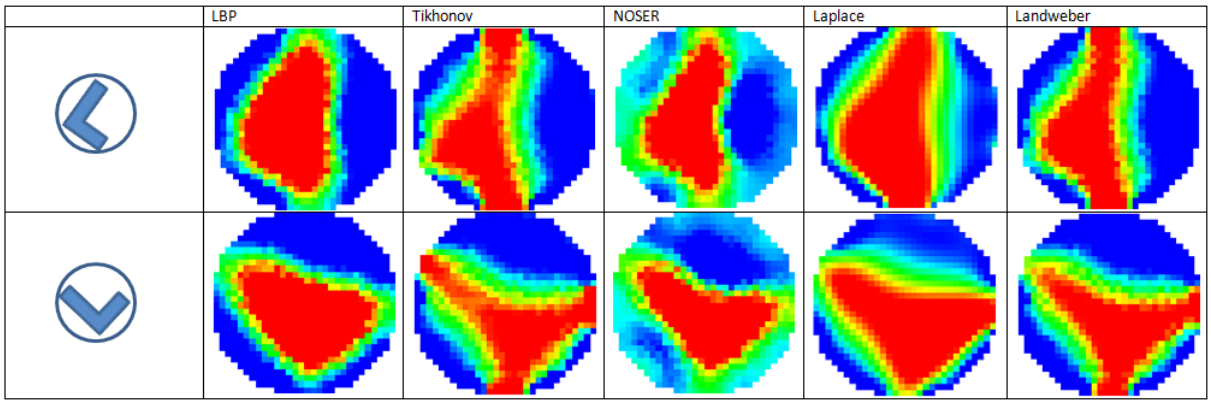

Figure 7: Inserting an L-shape object in an ECT sensor in different angles

3.2 ERT Experiments

The sensor used for ERT experiments is a 16 channel cylindrical container, with a diameter of 154 mm. Three 15mm diameter plastic cylindrical rods were equally spaced around the sensor boundary and moved towards the centre gradually. Figure 8 shows the reconstruction result for each algorithm.

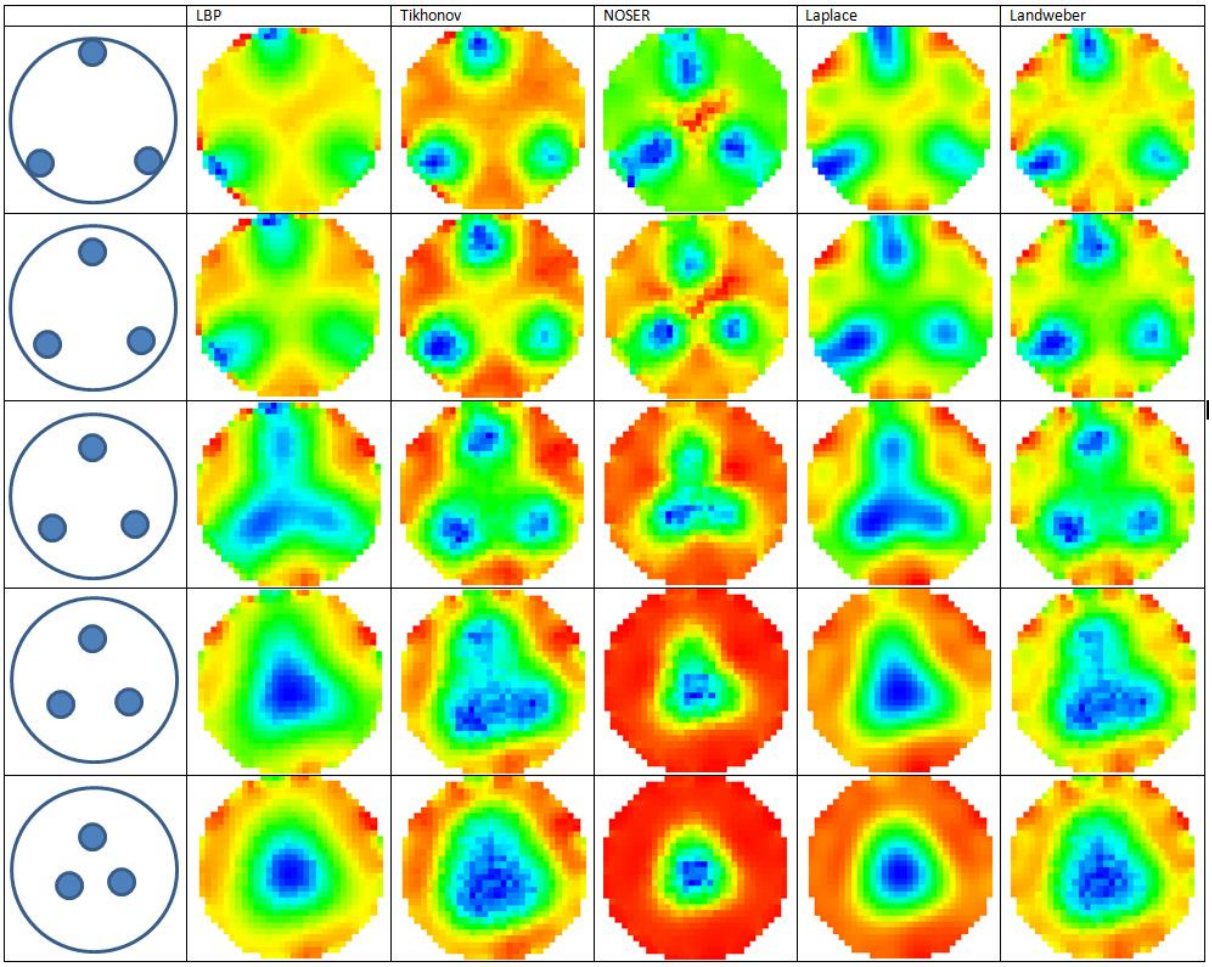

Figure 8: The algorithms' capability of separating three rods in an ERT sensor

4. EXPERIMENTAL VALIDATIONS – 3D

In this paper, ITS M3C ECT instrument and p2+ ERT instruments were used to conduct the 3D experiments. At this stage, the Reconstruction Tool-Suite software can only support 3D configurations of 3x8=24 channels for ECT and 2x16 = 32 channels for ERT. These two configurations will be the current standard configurations for ITS 3D ECT/ERT sensors. The sensor configurations will be expanded in the future. Figure 9 shows the experimental setup for both ERT and ECT tests.

Some initial tests were conducted using both 3D ERT and ECT sensors. The frame rate for 3D will be dramatically reduced due to the increased number of signal measurements (276 measurements per frame for ECT and 464 measurements per frame for ERT). For the standard instrumental setup, the frame rate would be decreased significantly to roughly 1 frame/sec, which is not suitable for real time processes. Since the designed experiments in this section are all for object detection, Tikhonov method is used for all the validation experiments in this Section.

Figure 9: (left) 3x8 ECT and (right) 2x16 ERT experimental setup

For the 3D ECT experiment, a filling process is monitored using a 3x8 ECT sensor. The sensor has a diameter of 95mm and a height of 150mm. An empty plastic vessel is first inserted at the centre of the ECT sensor when taking the reference signal. When the experiment starts, 500ml of polymer beads were added slowly into the plastic vessel continuously. This whole filling process took about 18 seconds was expected to be captured from our reconstructed 3D images.

A 140mm diameter ERT cylindrical sensor was used for 3D ERT experiments. Plastic pipes and rubber corks (non-conductive) were placed in various locations within a 2x16 ERT sensor. The reconstructed images are expected to show the location of the inclusions correctly. Figure 10 and 11 show the experimental results for 3D ERT and ECT using ITS p2+ and m3c systems.

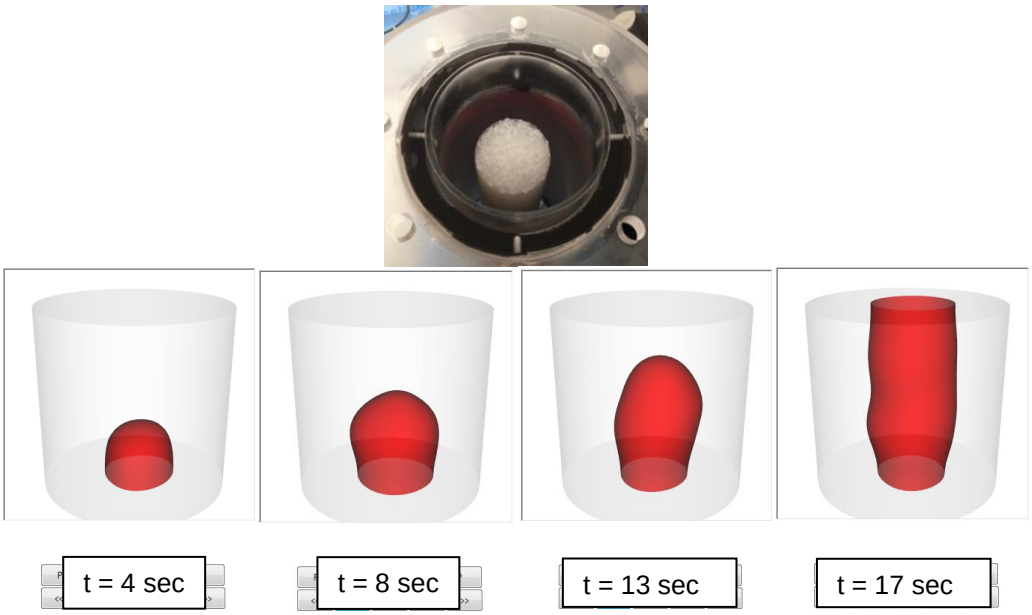

Figure 10: Using 3D ECT to monitor a polymer filling process

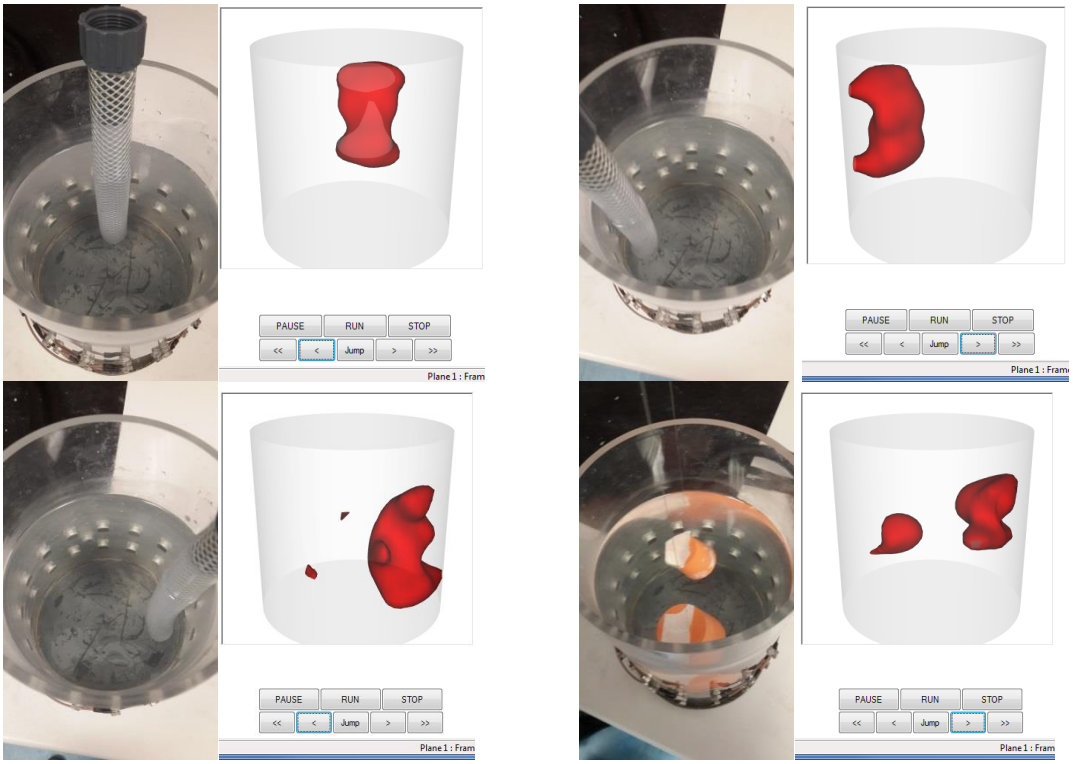

Figure 11: 3D ERT image reconstruction results, showing the locations of non-conductive objects

The biggest advantage of 3D reconstruction over 2D reconstruction is that it can provide extra axial information. When the processes involve variations along the z-axis, 3D configuration would be able to capture this information, and projected back to the 3D tomograms. Some experiments were designed to demonstrate the situations when the axial information is unsymmetrical and cannot be reproduced using 2D tomograms with axial interpolation algorithms. Figure 12 shows the results.

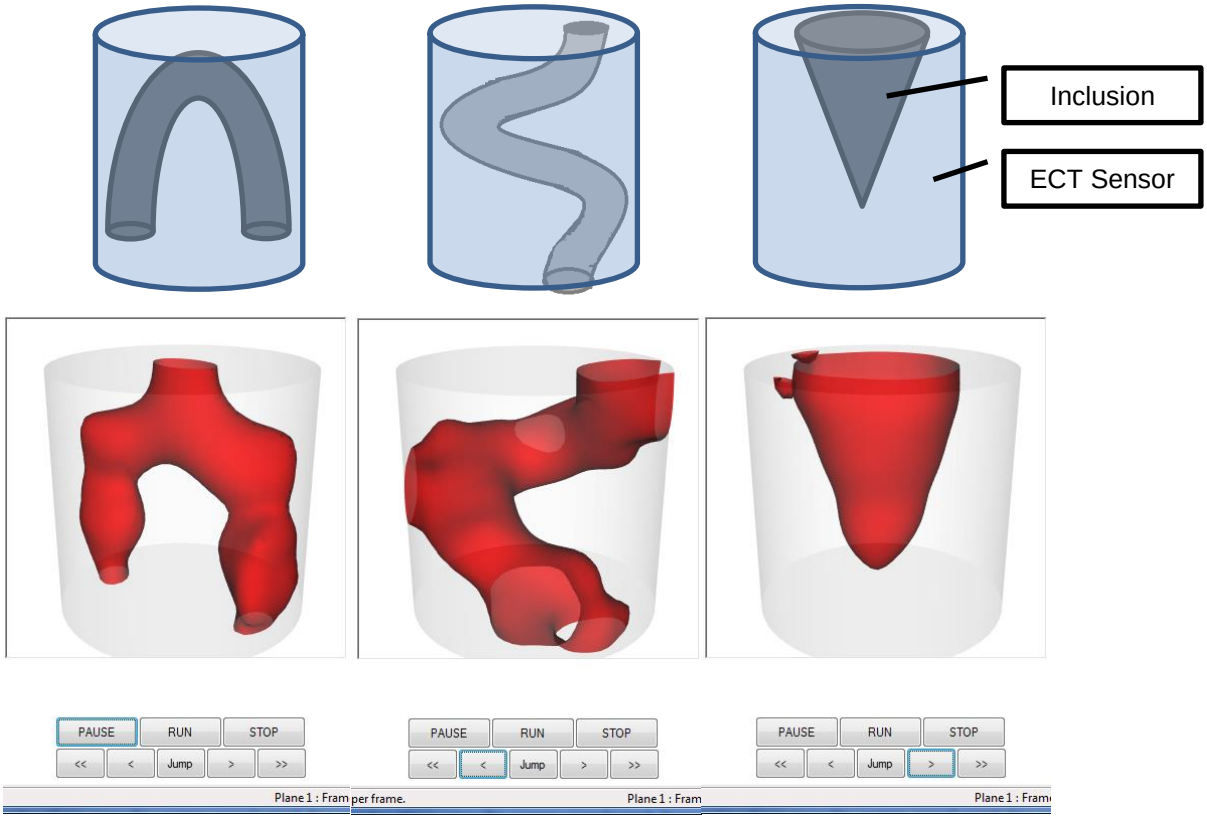

Figure 12: 3D Reconstruction with non-axial symmetrical inclusions: (left) U-shape, (middle) Helix-Shape and (right) Cone shape

5. IMAGE ANALYSIS RESULT

5.1 2D Reconstruction Result

From Figure 7, it can be seen that Tikhonov and Landweber methods performs the best in terms of shape recovery. For the interface level test (Figure 6), Laplace gives the most dispersed interface result; however all the other algorithms have similar performances. In the ERT experiments (Figure 8), Tikhonov and Landweber have a better resolution performance than LBP, NOSER and Laplace methods. In this particular experiment, Tikhonov method can improve the LBP resolution from 25% of the sensor diameter to 12%, i.e. the object can still be separated in the reconstructed image when the non-conducting rods is 19mm apart from each other.

5.2 3D Reconstruction Result

For From Figure 10, 11 and 12, the results demonstrate that the 3D reconstruction is achievable by using the existing ITS tomography instruments; the systems successfully capture the polymer bead filling process and also the location of the non-conducting materials (in tap water). The axial information of the unsymmetrical inclusion can also be successfully reconstructed, whereas it cannot be achieved by conventional 2D tomography. More analysis will be required to determine the accuracy of the three-dimensional images, however, the aim of this paper has been achieved, as the experimental results show that ITS instruments has the capability of doing full-field tomography. The data acquisition speed is the main constraint for real time visualisation, due to a large number of acquisition data. Some data reduction methods are proposed to eliminate this long acquisition time problem [Li 2013]. However this method cannot be implemented into the ordinary ITS instruments. System hardware needs to be re-configured to perform this data reduction method.

More sensor configuration will be added in the future, to broaden the user groups that can benefit from our 3D package. More work need to be done on 3D analysis. ITS believes that our latest 3D reconstruction scheme can offer our customers another platform to further understand their processes.

5.3 Algorithm Summary

By doing a series of tests, a summary table can be constructed. Table 3 gives the feature of all the algorithms integrated in the Reconstruction Tool-Suite package.

Reconstructed Methods	Features	Recommended Applications
LBP	• Fast and simple maths • Works better under homogenous condition • Less effective in object separation and sharp edge detection.	Batch mixing, inline mixing, batch to continuous reaction, slurry flow, homogenous processes.
Tikhonov (with Super Jacobian scheme)	• Regularised method (same speed as LBP) • Better performance on object separation and shape recovery applications. • Select unappropriated regularisation can ruin the reconstruction process.	Mixing, slurry flow, interface detection, multi-phase flow, bubble column, pneumatic flow, sharp edge detection applications.
NOSER (with Super Jacobian scheme)	• Regularised method (same speed as LBP) • The NOSER regularisation matrix is scaled based on the sensitivity map, i.e. less boundary effect • More noise tolerant	Applications with large noise and poor inter-plane sensitivity
Laplace (with Super Jacobian scheme)	• Regularised method (same speed as LBP) • The Laplacian filter is designed to penalise high frequency components in the image, i.e. the reconstructed image tends to be smoother • Less effective for sharp edge detection application	Batch mixing, inline mixing, batch to continuous reactions, homogenous processes
Landweber	• Iterative gradient descent method • Consume less memory resource than the single step method, but it is more time consuming • Similar performance to Tikhonov, i.e. more effective on object separation and shape recovery	Mixing, slurry flow, interface detection, multi-phase flow, bubble column, pneumatic flows, sharp edge detection applications.

Table 3: Summary of the algorithms integrated in Reconstruction Tool-Suite

6. CONCLUSION

In this paper, a reconstruction algorithm program is developed and presented to ITS system users. An overview of five different image reconstruction algorithms is discussed based on the experimental validations. In overall, LBP is still a very attractive method because of its simplicity, and its performance on homogenous distributed processes is better than the other regularised methods. However, when it comes to the process that involves sharp edge features, the regularised method like Tikhonov can offer a better imaging result that is closer to the real situation. The downside of these new algorithms is that the reconstruction processes require users to select an appropriate regularisation parameter, which complicates the reconstruction process. To overcome the difficulty, a table will be provided in the software manual so the regularisation parameters can be easily selected based on our benchmark experiments. It is important to know that different applications will have different suitable reconstruction methods.

Full-field 3D tomography models are also discussed and demonstrated in this paper using the Tool-Suite software. The advantage of 3D tomography is that its reconstruction takes inter-plane measurement into consideration, which can provide the electrical property distribution in the axial direction. In this case the reconstructed image can potentially reflect more detail about the processes. The downside of it is that more sensor measurements are required to reconstruct one tomogram image, i.e. the data acquisition time will be longer.

In general, ITS has developed this platform for the entire industrial tomography user to gain further insights of their processes. The software is compatible with Windows XP, Vista and 7 operation systems. The user can easily load the voltage measurement file and perform image reconstruction using various inverse algorithms embedded in the software. In the version 1.0 of the software, the image reconstruction supports both circular and square ERT and ECT geometries. More features and geometries will be included in the next version of the Reconstruction Tool-Suite software.

ACKNOWLEDGMENT

The authors would like to thank the UK Technology Strategy Board (TSB) for support of this work on the Knowledge Transfer Partnership (KTP) project (KTP009034).

REFERENCES

Henderson, R.P., Webster, J.G. (1978). "An Impedance Camera for Spatially Specific Measurements of the Thorax". IEEE Trans. Biomed. Eng. 25 (3), pages 250-254.

Barber, D.C.; Brown, B.H. (1984). "Applied Potential Tomography". J. Phys. E:Sci. Instrum 17 (9), pages 723-733.

Rodgers, T.L. and Kowalski, A. (2010). “An electrical resistance tomography method for determining mixing in batch addition with a level change”. Chemical Engineering Research and Design, 88, page 201-212.

Gamio J. C., Castro J., Rivera L., Alamillia J., Garcia-Nocetti F. and Aguilar L. (2005). “Visualisation of gas-oil two-phase flow in pressurised pipes using electrical capacitance tomography”. Flow Measurement and Instrumentation, Volume 16, page 129-134.

Giguére, R., Fradette, L., Mignon, D. and Tanguy, P.A. (2008). “Characterisation of slurry flow regime transitions by ERT”. Chemical Engineering Research and Design, Volume 86, page 989-996.

Wang, M. (1999). “Three- dimensional Effects in Electrical Impedance Tomography”. 1st World Congress on Industrial Process Tomography, page 410-415.

Davidson, J. L., Ruffino, L. S., Stephenson, D. R., Mann, R., Grieve, B. D. and York, T. A. (2004). “Three-dimensional electrical impedance tomography applied to a metal-walled filtration test platform”. Measurement Science and Technology. Volume 15, number 11.

Soleimani, M. (2006), “Three-dimensional electrical capacitance tomography imaging. Insight: Non-Destructive Testing and Condition Monitoring”, 48 (10), page 613-617.

R Wajman, R Banasiak, L Mazurkiewicz, T Dyakowski and D Sankowski (2006), “Spatial imaging with 3D capacitance measurements”, Meas. Sci. Technol. 17 2113

Fan, L.S., Warsito, W. and Marashdeh, Q. (2007). "Electrical capacitance volume tomography." IEEE SENSORS JOURNAL Volume 7 3-4, page 525-535.

Banasiak, R. and Soleimani, M. (2010). Shape based reconstruction of experimental data in 3D electrical capacitance tomography. NDT & E International, 43 (3), page 241-249.

Sun, J. and Yang, W. (2012). “3D effect of electrical capacitance and resistance tomography sensors”. Imaging Systems and Techniques, page 562-566.

Yan, H., Lu, Y. and Wang, Y. (2013). “3D Reconstruction and Visualization of Volume Data in Electrical Capacitance Tomography”. Journal of Software, Volume 8, number 10, page 2529-2534.

Ye, L. and Yang, W. Q. (2012). “Real-time 3D Visualisation in Electrical Capacitance Tomography”. IEEE International Conference on Imaging Systems and Techniques (IST). Page 40-44.

Lionheart W.R.B. (2004). “EIT reconstruction algorithms: pitfalls, challenges and recent developments, Physiological Measurement”. Volume 25, page 125-142.

Soleimani, M. and Lionheart, W. R. B. (2005). “Nonlinear image reconstruction for electrical capacitance tomography experimental data using experimental data”. Measurement Science & Technology, 16 (10), page 1987-1996.

Soleimani, M., Wang. H., Li Y. and Yang, W. Q. (2007). “A comparative study of 3D electrical capacitance tomography”. International journal of information and systems sciences, volume 3, number 2, page 292-306.

Marashdeh, Q. and Teixeira, F. L. (2004), “Sensitivity matrix calculation for fast 3-D electrical capacitance tomography (ECT) of flow systems”, IEEE Transactions on Magnetics, Volume 40, Issue 2, page 1204-1207.

Xu. G., Wu, H., Yang, S., Liu, S., Li, Y.,Yang, Q.,Yan, W. and Wang M. (2005). “3-D Electrical Impedance Tomography Forward Problem with Finite Element Method”. IEEE Trans. On Magnetics. Volume 41, number 5, page 1832-1835.

Yang W. Q. and Peng L. (2003). “Image reconstruction algorithms for electrical capacitance tomography, Measurement Science and Technology”, Volume 14, R1 – R13.

Cheney, M, Isaacson D, Newell, J.C., Simske, S. and Goble, J. (1990). “NOSER: An algorithm for solving the inverse conductivity problem”. International Journal of Imaging Systems and Technology, Volume 2, page 66-75.

Dai, T., Soleimani, M. and Adler, A. (2008), “EIT image reconstruction with four dimensional regularization”. Medical & Biological Engineering & Computing, 46 (9), page 889-899

Adler A. and Lionheart, W. R. B. (2006). “Uses and abuses of EIDORS: an extensible software base for EIT”. Physiological Measurement ,Volume 27, Number 5.

LAPACK – Linear Algebra PACKage, http://www.netlib.org/lapack/, Last updated on 16th Nov 2013. Visited on 30th Oct 2014.

Armadillo – C++ linear algebra library, http://arma.sourceforge.net/. Last updated on 30th Oct 2014. Visited on 30th Oct 2014.

Eigen, http://eigen.tuxfamily.org/. Last updated 20th Oct 2014. Visited on 30th Oct 2014.

Adler, A., Dai, T. and Lionheart, W. R. B. (2007). “Temporal Image Reconstruction in Electrical Impedance Tomography”. Physiol. Meas. Volume 28, number 7.

Li, Y. and Holland, D. J. (2013). “Fast and robust 3D electrical capacitance tomography”. Measurement Science and Technology. Volume 24, number 10.